



GEOARENA: AN OPEN PLATFORM FOR BENCHMARKING LARGE VISION-LANGUAGE MODELS ON WORLDWIDE IMAGE GEOLOCALIZATION

Pengyue Jia^{1,2*}, Yingyi Zhang^{1*}, Xiangyu Zhao¹, Yixuan Li²

¹Department of Data Science, City University of Hong Kong

²Department of Computer Sciences, University of Wisconsin-Madison

{jia.pengyue, yzhang6375-c}@my.cityu.edu.hk

xianzhao@cityu.edu.hk, sharonli@cs.wisc.edu

*Equal contribution

<https://huggingface.co/spaces/garena2/GeoArena>

ABSTRACT

Image geolocalization aims to predict the geographic location of images captured anywhere on Earth, but its global nature presents significant challenges. Current evaluation methodologies suffer from two major limitations. First, data leakage: advanced approaches often rely on large vision-language models (LVLMs) to predict image locations, yet these models are frequently pretrained on the test datasets, compromising the accuracy of evaluating a model’s actual geolocalization capability. Second, existing metrics primarily rely on exact geographic coordinates to assess predictions, which not only neglects the reasoning process but also raises privacy concerns when user-level location data is required. To address these issues, we propose **GeoArena**, *a first open platform for evaluating LVLMs on worldwide image geolocalization tasks, offering true in-the-wild and human-centered benchmarking*. GeoArena enables users to upload in-the-wild images for a more diverse evaluation corpus, and it leverages pairwise human judgments to determine which model output better aligns with human expectations. Our platform has been deployed online for two months, during which we collected over thousands voting records. Based on this data, we conduct a detailed analysis and establish a leaderboard of different LVLMs on the image geolocalization task.

1 INTRODUCTION

Image worldwide geolocalization is a highly challenging task that lies at the intersection of computer vision (Szeliski, 2022; He et al., 2016) and geographic artificial intelligence (Mai et al., 2022). It aims to pinpoint the exact location on Earth where a given image was taken. This task has significant application potential, such as in navigation, positioning, crime tracking, and disaster monitoring. Despite its broad utility, geolocalization remains a hard problem due to the enormous variability in visual appearances across the globe, coupled with the need for fine-grained spatial reasoning.

Recently, advanced methods for image worldwide geolocalization have increasingly relied on powerful large vision-language models (LVLMs) to generate predictions (Vivanco Cepeda et al., 2023; Zhou et al., 2024; Jia et al., 2024). To assess the performance of different methods on geolocalization tasks, the research community has proposed a series of benchmark studies (Li et al., 2025; Huang et al., 2025; Jay et al., 2025; Liu et al., 2024; Wang et al., 2024; Astruc et al., 2024). Without exception, these benchmarks are based on static datasets and evaluate model performance using ground-truth labels (i.e., by calculating the distance between the predicted GPS location and the ground-truth GPS), as shown in Table 1. This evaluation approach is efficient and requires relatively few resources. However, it has two notable limitations: (1) Data leakage: Static test datasets are inevitably subject to data leakage, meaning that the test data may be included in the pretraining data of LVLMs; and (2) GPS-based evaluation: Existing evaluations only consider the spatial distance between the final prediction and the ground truth, ignoring the model’s reasoning process. This can lead to cases where

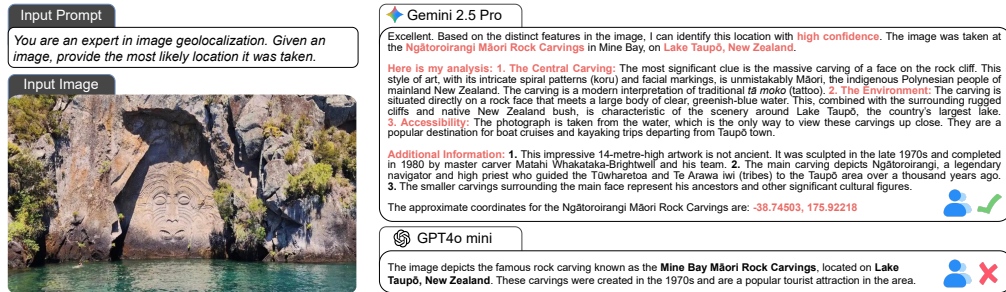


Figure 1: Example of geolocalization: identifying the Ngātoroirangi Māori Rock Carvings.

Table 1: Comparison with different benchmarks on different properties.

Benchmarks	OSV-5M	LLMGeo	ETHAN	Location-Inference	FairLocator	IMAGEO-Bench	GeoArena
Conference Reference	CVPR'24 Astruc et al. (2024)	CVPR'24 Wang et al. (2024)	Arxiv'24 Liu et al. (2024)	AAAI'25 Jay et al. (2025)	Arxiv'25 Huang et al. (2025)	Arxiv'25 Li et al. (2025)	-
Evaluation	GPS	Country	GPS	GPS, Country, City	GPS, Street, City, Country, Continent	GPS, City, State, Country	Ours
Live	X	X	X	X	X	X	
Privacy-Preserving	X	X	X	X	X	X	✓

models with flawed reasoning processes achieve higher scores by chance when they predict closer to the ground truth. Moreover, relying on exact geographic coordinates for evaluation raises privacy concerns, since it requires access to sensitive user-level location data. To address these limitations and develop a more effective evaluation approach, it is necessary to build a *dynamic and human-centered benchmarking platform that can capture the real-world challenges of image geolocalization*.

Designing such an evaluation platform is inherently challenging. It involves gathering a steady stream of diverse and representative user images that capture the variability of real-world conditions. Furthermore, the platform must support scalable and efficient evaluation pipelines capable of handling a wide range of model submissions. Finally, designing a reasonable model ranking system based on user preferences is also essential. These challenges highlight the need for careful design and robust infrastructure to create a meaningful and practical benchmarking platform for image geolocalization.

To this end, we introduce **GeoArena**, an open platform for benchmarking Large Vision-language Models on worldwide image geolocalization. GeoArena addresses two critical issues in current evaluation practices. First, GeoArena collects in-the-wild images contributed by real-world users, ensuring data diversity and dynamic updates, which help mitigate data leakage from static datasets. Second, GeoArena employs human preferences to assess the quality of model predictions, moving beyond sole reliance on GPS accuracy and mitigating the privacy risks associated with requiring exact user location data. Through these improvements, GeoArena establishes a new evaluation framework for image geolocalization that is more dynamic, privacy-preserving, and reflective of real-world user experience. This approach bridges the gap between automated metrics and human-centered evaluation, providing a more robust and generalizable benchmark for the community. Specifically, when a user enters GeoArena and submits an image for geolocalization, two anonymous models each generate a response indicating the predicted location. The user then votes on which response is more satisfactory. After collecting a large volume of voting data, we apply statistical methods to generate reliable rankings for all models. These rankings can serve as valuable references for users in the field, guiding them in selecting models that best align with geolocalization needs.

GeoArena has been successfully deployed since June 2025, operating for over two months and collecting thousands of records. Our deployment has already revealed clear patterns: frontier systems like Gemini-2.5 dominate the leaderboard, while strong open-source families such as Qwen2.5 and Gemma-3 are closing the gap. User preference analysis shows that longer and more structured responses are consistently favored, highlighting the importance of reasoning quality. We also find that top proprietary models align more closely with human judgment than open-source counterparts, though noticeable gaps remain. These insights demonstrate GeoArena’s ability to both benchmark models dynamically and uncover the factors that shape human evaluations in geolocalization. We will release all the collected voting data to support advancements in related areas, such as reward modeling and geographic foundation models. Our key contributions can be summarized as follows:

1. We develop GeoArena, the first live, user-preference-based open platform for evaluating Large Vision-language Models on image worldwide geolocalization.
2. We conduct a comprehensive analysis of the collected user inputs and voting data to demonstrate the reliability and capabilities of GeoArena.
3. We publicly release the collected prompts, images, and voting data to support research and development in related fields such as reward modeling and geographic foundation models.

2 RELATED WORK

Image Worldwide Geolocalization. Image worldwide geolocalization is an interdisciplinary task that bridges geography and computer science, involving GeoAI, spatial data mining (Wang et al., 2020), and multi-modal modeling (Wang et al., 2023). In recent years, thanks to the strong world knowledge and visual understanding capabilities of large vision-language models (LVLMs), image geolocalization has made significant progress (Li et al., 2024; Haas et al., 2024). Methodologically, GeoCLIP (Vivanco Cepeda et al., 2023) leverages the CLIP architecture to separately model images and GPS coordinates, retrieving the GPS candidate closest to the image’s representations through vector similarity matching. Img2Loc (Zhou et al., 2024) is the first to introduce LVLMs into image geolocalization, retrieving similar images’ information and incorporating it as prompts into the LVLM input to utilize the world knowledge acquired during pretraining to predict the image’s location. G3 (Jia et al., 2024) further improves upon Img2Loc by optimizing both the image retrieval and reasoning processes, enabling the model to obtain more accurate reference information and fully exploit the prediction potential of LVLMs.

Benchmark of Geolocalization. Common evaluation datasets used in geolocalization task include IM2GPS (Hays & Efros, 2008) and YFCC (Thomee et al., 2016). On the benchmarking side, LLMGeo (Wang et al., 2024) collects datasets from Google Street View and evaluates LVLMs. Liu et al. (2024) evaluates the performance of LVLMs on IM2GPS and YFCC and shows that incorporating chain-of-thought (CoT) (Wei et al., 2022) reasoning can improve performance on geolocation tasks. Jay et al. (2025) also extracts data from Google Street View to create a more generalized evaluation set, finding that VLMs already outperform the average human baseline in geolocation capabilities. FairLocator (Huang et al., 2025) evaluates LVLMs’ urban geolocation abilities and focuses on biases in the geolocation capabilities of VLMs. In contrast to these methods and benchmark studies, we propose GeoArena, the *first live and user-preference-based benchmark for image geolocalization*. GeoArena collects in-the-wild images uploaded by users, effectively mitigating the data leakage issues of static datasets while also avoiding the privacy risks associated with requiring exact GPS annotations. In addition, the image distribution in GeoArena is more representative of real-world use cases, and the platform uses user preferences to generate rankings of model capabilities. This provides a more robust and user-aligned evaluation framework for image worldwide geolocalization.

Large Vision-language Models. Large language models (LLMs) have recently shown impressive generalization across diverse tasks, achieving state-of-the-art results in areas ranging from reasoning to text generation (Zhao et al., 2023). However, their unimodal nature limits their ability to process visual input, motivating the development of large vision-language models (LVLMs). For example, LLaVA (Liu et al., 2023) blends visual and linguistic information for instruction-following tasks. Qwen2.5-VL (Bai et al., 2025) extends LVLMs with dynamic-resolution visual processing, precise object grounding, and structured document parsing. In our work, GeoArena focuses on evaluating LVLMs that generate text predictions conditioned on images, specifically assessing their ability to perform geolocalization. This benchmark offers users contextual guidance in GeoAI applications and complements existing evaluations by concentrating on geographic prediction performance.

3 GEOARENA

GeoArena is an interactive platform designed to evaluate the geolocalization capabilities of various LVLMs. In this section, we provide a detailed description of GeoArena, including its live interface (Section 3.1), data collection process (Section 3.2), the models it encompasses (Section 3.3), and the ranking computation methods (Section 3.4).

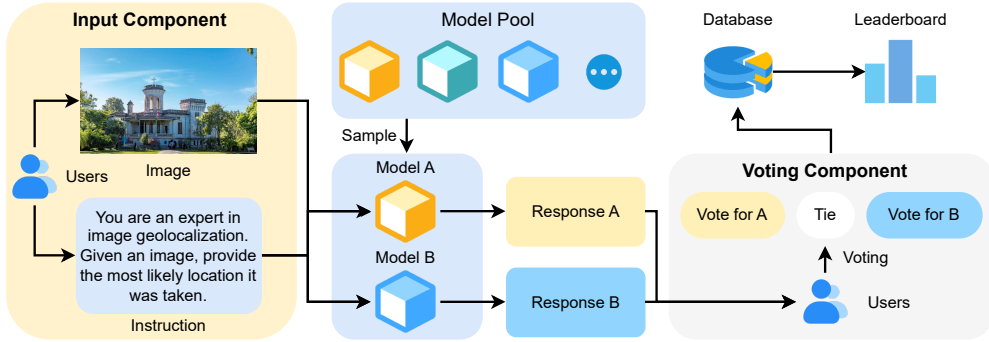


Figure 2: Overview of GeoArena.

3.1 LIVE INTERFACE

To facilitate user interaction, GeoArena is an online platform that allows any user to conveniently access the leaderboard and participate in data collection through a public link. As shown in Figure 2, the live interface consists of two main components: an input component and a voting component. (1) The input component includes both an image input and a prompt input. Users can upload images that they wish to geolocate, while the prompt input allows users to specify personalized geolocation instructions. To improve efficiency, we also provide a default instruction derived from previous work (Zhou et al., 2024; Jia et al., 2024). (2) The voting component displays two side-by-side outputs generated by two anonymized models that are automatically sampled. After clicking the submit button, three voting options pop up: “vote for left”, “vote for right”, and “tie” (indicating comparable quality between the two outputs). Once the user submits a vote, the true model identities are revealed to maintain user impartiality during the voting process.

3.2 DATA COLLECTION

GeoArena collects essential data for each evaluation session to enable rigorous analysis and reliable leaderboard computation. For every voting event, we record the names of the two models being compared, the winning model, the user-provided prompt, the uploaded image, the generated responses, and the timestamp of the interaction. This information ensures the traceability of each comparison, supports the calculation of rankings, and allows for reproducible experiments. All data are stored in structured JSON files, which facilitate downstream analysis and leaderboard generation. To preserve user privacy, we anonymize user inputs and apply filters to remove any potentially sensitive or inappropriate content.

3.3 PARTICIPATING MODELS

To ensure comprehensive and meaningful comparisons, GeoArena includes a wide range of both open-source and proprietary models. Our selection covers popular large vision-language models from multiple providers. For the GPT series (Achiam et al., 2023), we include GPT-4o, GPT-4o-mini, GPT-4.1, GPT-4.1-mini, and GPT-4.1 Nano. From the Gemini family (Team et al., 2023), we incorporate Gemini 2.5 pro and Gemini 2.5 flash. The Claude series includes Claude Opus 4 and Claude Sonnet 4. We also evaluate Llama 4 Maverick and Llama4 Scout (Touvron et al., 2023), as well as Gemma 3 models (Team et al., 2025) in sizes of 27B, 12B, and 4B. Additionally, our platform features Qwen2.5-VL models in sizes of 72B, 32B, 7B (Bai et al., 2025). In total, GeoArena currently benchmarks 17 models. This broad coverage ensures that users and researchers can evaluate model performance across different architectures, training paradigms, and capabilities.

3.4 RANKING COMPUTATION METHODS

Online Elo Ranking. The Elo rating system is a widely used approach to estimate the relative strength of different models or players based on pairwise comparisons. Originally introduced for

Table 2: Large-scale models benchmarked in *GeoArena*. Prices are USD / million tokens (input/output) and USD / thousand (image).

Model	Company	Params	Openness	API Price (input / output / image)
GPT-4o	OpenAI 	Unknown	Proprietary	\$2.50 / \$10.00 / \$3.61
GPT-4o-mini	OpenAI 	Unknown	Proprietary	\$0.15 / \$0.60 / \$0.22
GPT-4.1	OpenAI 	Unknown	Proprietary	\$2.00 / \$8.00 / -
GPT-4.1-mini	OpenAI 	Unknown	Proprietary	\$0.40 / \$1.60 / -
GPT-4.1 Nano	OpenAI 	Unknown	Proprietary	\$0.10 / \$0.40 / -
Gemini 2.5 Flash	Google DeepMind 	Unknown	Proprietary	\$0.15 / \$0.60 / \$0.62
Gemini 2.5 Pro	Google DeepMind 	Unknown	Proprietary	\$1.25 / \$10.00 / \$5.16
Claude Sonnet 4	Anthropic 	Unknown	Proprietary	\$3.00 / \$15.00 / \$4.80
Claude Opus 4	Anthropic 	Unknown	Proprietary	\$15.00 / \$75.00 / \$24.00
Llama 4 Maverick	Meta 	17B/402B	Open-source	\$0.15 / \$0.60 / \$0.67
Llama 4 Scout	Meta 	17B/109B	Open-source	\$0.08 / \$0.30 / -
Gemma 3 27B	Google 	27B	Open-source	\$0.10 / \$0.20 / \$0.03
Gemma 3 12B	Google 	12B	Open-source	\$0.15 / \$0.10 / -
Gemma 3 4B	Google 	4B	Open-source	\$0.02 / \$0.04 / -
Qwen 2.5-VL 72B	Alibaba 	72B	Open-source	\$0.25 / \$0.75 / -
Qwen 2.5-VL 32B	Alibaba 	32B	Open-source	\$0.90 / \$0.90 / -
Qwen 2.5-VL 7B	Alibaba 	7B	Open-source	\$0.20 / \$0.20 / -

ranking chess players, it has been extended to various evaluation tasks in machine learning and artificial intelligence. Elo rating provides an interpretable score that reflects the expected probability of one model outperforming another.

Formally, given two models i and j with Elo ratings R_i and R_j , the expected probability that model i will outperform model j is defined as:

$$E(i, j) = \frac{1}{1 + 10^{(R_j - R_i)/\alpha}} \quad (1)$$

where α is a scaling parameter that controls the spread of the probability function, typically set to 400 in most implementations.

After observing the actual outcome $S(i, j)$, where $S(i, j) = 1$ if model i wins, $S(i, j) = 0.5$ for a tie, and $S(i, j) = 0$ if model i loses, the Elo rating of model i will be updated as:

$$R'_i = R_i + K \cdot (S(i, j) - E(i, j)), \quad (2)$$

where K is a learning rate that determines how quickly the rating adapts to new results. In our implementation, we collect all pairwise comparison outcomes from the user evaluations, and iteratively apply the above update rule to compute the Elo rating for each model.

From the above description, we can summarize two key features of the Elo rating system. First, it can operate without requiring a complete history of past matches, updating each model's rating using only its current Elo rating and the outcome of its most recent match. Second, the Elo rating system inherently assumes that the strength of each participant changes over time, rather than remaining constant. However, in the context of evaluating LVLMs, we generally assume that model capabilities are static. Furthermore, Elo ratings are more strongly influenced by recent matches, making them highly sensitive to the order of matches—an effect that is undesirable in our setting. To address this, we follow prior work (Chiang et al., 2024) and apply the Bradley-Terry model (Bradley & Terry, 1952) to estimate the final Elo ratings for each model on the image geolocalization task, ensuring a stable and order-invariant ranking.

Bradley-Terry Model. The Bradley-Terry (BT) model provides a principled way to estimate the relative strength of competing models through pairwise comparisons. In this framework, each model i is assigned a latent strength parameter R_i . The probability that model i outperforms model j is given by:

$$P(i > j) = \frac{1}{1 + 10^{(R_j - R_i)/\alpha}}, \quad (3)$$

where α is a scaling parameter (typically set to 400) that controls the spread of probabilities. The BT model estimates the parameters R_i by maximizing the likelihood of all observed pairwise outcomes, accounting for repeated comparisons through a weighting term W_{ij} . The likelihood function is defined as:

$$\mathcal{L}(\mathbf{R}) = \sum_{i,j \in N, i \neq j} W_{ij} \log \left(\frac{1}{1 + 10^{(R_j - R_i)/\alpha}} \right) \quad (4)$$

To compute the final Elo ratings, we apply a linear transformation to align the model scores with the Elo rating scale. Specifically, after fitting the BT model via logistic regression, the estimated parameters \hat{R}_i are transformed as:

$$\text{Elo}_i = \text{scale} \cdot \hat{R}_i + \text{init_rating}, \quad (5)$$

where `scale` is typically set to 400 and `init_rating` is set to 1000. This transformation preserves the relative ranking among models while making the scores more interpretable and consistent with standard Elo rating conventions.

Confidence Interval. To ensure that the model ranking results are not overly dependent on a particular sample of comparisons, we estimate confidence intervals (CIs) for the elo scores. Specifically, we adopt a bootstrap procedure similar to the methodology employed in Chatbot Arena (Chiang et al., 2024), which repeatedly resamples the battle outcomes and re-computes the rating estimates. This approach allows us to quantify the variability in model rankings and provides statistically grounded intervals around each estimate. The inclusion of confidence intervals is essential because it enables us to distinguish between meaningful performance differences and those that may arise due to sampling noise. As a result, our reported rankings are not only more robust but also more interpretable from a statistical perspective, offering stronger evidence of the relative strengths of different LVLMs on the image geolocalization task.

3.5 GEOARENA-1K DATASET

Based on the data collected through GeoArena, we further release the **GeoArena-1K** dataset. This dataset consists of samples each containing the user-uploaded image, the textual instructions, pairwise model responses, the names of the competing models, and the corresponding human voting outcomes. To the best of our knowledge, this is the first human preference dataset for LVLMs in the domain of image geolocalization. Beyond serving as a preference dataset on image geolocalization, GeoArena-1K provides a valuable resource for advancing research in reward modeling and the development of geographic foundation models. More details about the GeoArena-1K dataset are illustrated in Appendix A.1.

4 BENCHMARKS AND RESULTS ANALYSIS

4.1 ARENA LEADERBOARD

Table 3 presents the GeoArena leaderboard as of September 2025, from which several key observations can be drawn: (1) Gemini models from DeepMind achieve the strongest performance, with Gemini-2.5-pro (Elo 1319.7) and Gemini-2.5-flash (Elo 1206.5) clearly outperforming all other systems. This highlights the advantage of large-scale, production-level multimodal pre-training in the challenging image geolocalization task. (2) Open-source families such as Qwen2.5 and Gemma-3 obtain competitive rankings. For example, Qwen2.5-VL-72B-Instruct (Elo 1094.5) surpasses Gemma-3-12B-it (Elo 1086.5) and performs comparably to the GPT-4.1 series, suggesting that open-source initiatives are rapidly narrowing the gap with proprietary frontier systems. (3) Several models, including LLaMA-4-Maverick, GPT-4.1, and Claude-Opus-4, cluster within the Elo 1040-1050 range. Their confidence intervals overlap substantially, indicating no statistically significant differences between these models. (4) Smaller variants such as GPT-4.1-nano, GPT-4o-mini, and the lightweight Qwen model (Qwen-2.5-VL-7B-Instruct) exhibit clear performance degradation, with ratings below 960. This underscores the inherent difficulty of image geolocalization, where reduced model capacity limits generalization across diverse global contexts on the challenging image geolocalization task. (5) The wide rating spread (1320 down to 871) validates the discriminative power of GeoArena. It provides a reliable platform to distinguish frontier-level systems from lightweight baselines, which is crucial for advancing research on geospatial reasoning in LVLMs.

Table 3: GeoArena Leaderboard in September 2025.

Ranking	Model	ELO Rating	95% CI lower	95% CI upper
0	google/gemini-2.5-pro	1319.7	974.8	1443.8
1	google/gemini-2.5-flash	1206.5	1062.2	1330.6
2	qwen/qwen2.5-vl-72b-instruct	1094.5	982.6	1181.9
3	google/gemma-3-12b-it	1086.5	1002.6	1186.4
4	google/gemma-3-27b-it	1065.5	959.3	1159.8
5	openai/gpt-4.1-mini	1059.8	970.0	1161.4
6	meta-llama/llama-4-maverick	1046.6	944.6	1115.3
7	qwen/qwen2.5-vl-32b-instruct	1044.8	964.9	1119.0
8	openai/gpt-4.1	1044.8	964.9	1119.0
9	anthropic/claude-opus-4	1042.3	933.8	1130.0
10	google/gemma-3-4b-it	1027.3	936.3	1102.0
11	anthropic/claude-sonnet-4	1019.9	921.3	1113.8
12	openai/gpt-4o	1000.0	1000.0	1000.0
13	meta-llama/llama-4-scout	984.2	876.0	1077.1
14	qwen/qwen-2.5-vl-7b-instruct	950.9	868.4	1056.2
15	openai/gpt-4.1-nano	917.9	819.1	1015.5
16	openai/gpt-4o-mini	871.6	715.2	1114.7

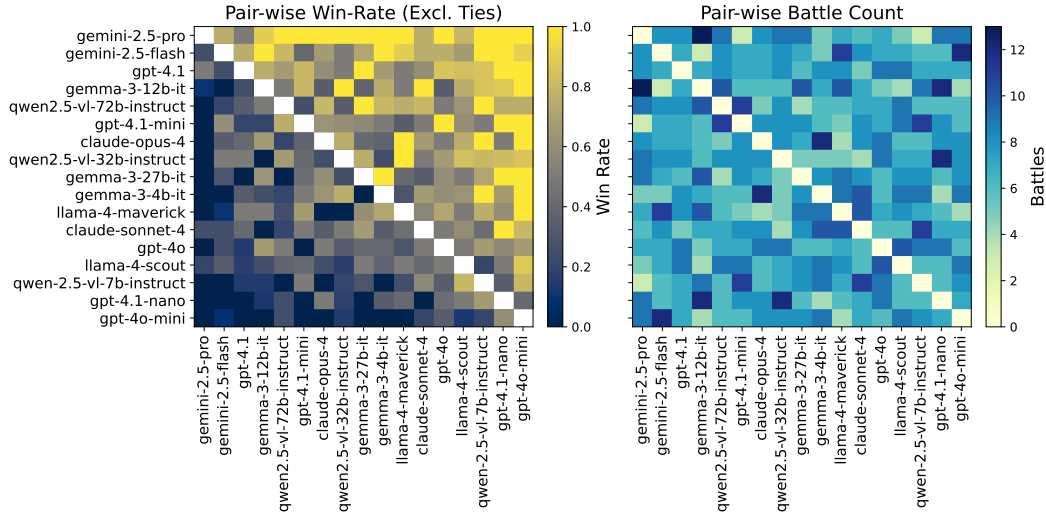


Figure 3: Pair-wise Performance Comparison of Models (Win-Rate and Battle Count).

4.2 BATTLE DATA ANALYSIS

To provide a comprehensive view of comparative model performance, we conduct a pair-wise analysis of model battles, reporting both win-rates and battle counts. Figure 3 reports a pair-wise comparison across models, with the left panel showing head-to-head win rates (ties excluded) and the right panel showing the corresponding battle counts. Models are ordered by their average win rate, which makes the block structure of the heatmap interpretable. We can find: **(1) Frontier models consistently dominate.** gemini-2.5-pro, gemini-2.5-flash, and gpt-4.1 occupy the top rows, maintaining win rates close to or above 0.7 against nearly all competitors. Their advantage is not limited to small baselines but extends to strong models from other families, suggesting that both model capacity and advanced alignment procedures contribute to their robustness. **(2) Mid-scale systems show transitional behavior.** Models such as gemma-3-12b-it, qwen2.5-vl-72b-instruct, and gpt-4.1-mini occupy the middle tier. They achieve favorable outcomes against smaller instruction-tuned variants but exhibit substantial performance gaps when challenged by the frontier tier. This

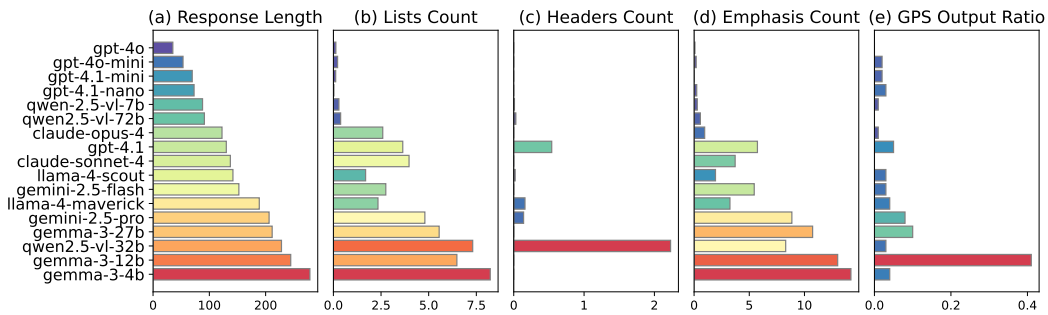


Figure 4: Distribution of Style Features in Model Outputs.

Table 4: Estimated Influence of Style Features on User Preference. A higher coefficient (β) for a style feature indicates that this attribute contributes more positively to user preference.

Features	Response Length	Lists Count	Headers Count	Emphasis Count	GPS Output Ratio
Coefficient β	0.526	0.095	-0.153	-0.117	0.06

indicates a stepwise stratification that correlates with effective model size and tuning intensity. (3) **Lower-capacity models underperform broadly.** Systems including gemma-3-4b-it, qwen2.5-vl-7b-instruct, gpt-4.1-nano, and gpt-4o-mini cluster near the bottom of the heatmap, with win rates typically below 0.3 against larger peers. Their deficits are systematic across families, reflecting limited parameter budgets and less extensive post-training data. (4) **Family-specific patterns emerge.** Within families, performance scales predictably with size. For example, the qwen2.5-vl series shows clear gains moving from 7B to 72B parameters, while the gemma-3 series shows improvements from 4B to 27B. These intra-family trends suggest that scaling and alignment strategies jointly determine competitiveness. (5) **Reliability depends on comparison frequency.** The right panel shows that battle counts are not uniform across pairs. Matchups with a large number of battles provide more reliable evidence, as the corresponding win-rate contrasts are better supported by data. In contrast, extreme win rates observed in sparsely sampled cells should be interpreted with caution. As voting accumulates over time, our leaderboard becomes increasingly stable, reflecting consistent patterns across many opponents and repeated battles.

4.3 PREFERENCE ANALYSIS

To better understand which characteristics of model responses drive user preference, following previous work (Chiang et al., 2024; Tianle Li, 2024; Dubois et al., 2024), we extend the standard Bradley-Terry regression framework by incorporating style-related features as confounding variables. In practice, this means that for each model comparison, we not only encode which two models are being compared, but also include additional features that describe the differences in response style, such as normalized response length, number of lists, headers, emphasis markers, or the ratio of GPS outputs. By including these features in the regression, we can separate the effect of style from the intrinsic ability of the model. The resulting model coefficients therefore capture a model’s underlying strength, while the style coefficients quantify how much specific stylistic traits influence user choices. A higher coefficient (β) for a style feature indicates that this attribute contributes more positively to user preference. In this study, we primarily consider five different style features: response length (measured by the number of words), lists count (including both unordered and ordered lists), headers count, emphasis count (including the number of bold and italic items), and GPS output ratio (the proportion of responses containing GPS-level predictions). Figure 4 illustrates the distribution of these features across different models, showing clear stylistic variation in model outputs. From the experimental results in Table 4, we observe consistent findings with prior work (Chiang et al., 2024; Steyvers et al., 2024; Tianle Li, 2024): response length exhibits a strong positive correlation with human preference (i.e., $\beta_{\text{response}} = 0.526$), as longer responses are more likely to be favored by users. In addition, both lists count ($\beta_{\text{list}} = 0.095$) and GPS output ratio ($\beta_{\text{GPS}} = 0.06$) are positively correlated with preference, where a higher number of lists often reflects more explicit

Table 5: Alignment accuracy of LLMs with human judgments on sampled response pairs.

Model	Gemini 2.5 Pro	Qwen2.5-VL-72B
Accuracy	0.6579	0.4667

reasoning steps, and GPS outputs provide finer-grained and more concrete answers. However, headers count and emphasis count do not show positive associations with human preference. A possible explanation is that excessive use of structural markers or textual emphasis may be perceived as superficial formatting rather than substantive content, and thus does not contribute to the perceived quality or informativeness of the response.

4.4 ALIGNMENT STUDY BETWEEN LVLM AND USER

To further examine whether LVLMs can serve as reliable judges for geolocalization responses, we conduct an alignment study that compares LLM preferences with human annotations. Specifically, we randomly sample 100 response pairs from the dataset. For each pair, we ask an LVLM to decide which response (generated by Model A or Model B) is better in terms of accuracy, reasoning, and clarity, and require the model to output only one of three labels: win, tie, or loss. The prompt template we used is shown in Appendix A.2.

We then compute the agreement accuracy between the LVLM’s judgment and the human-provided ground truth labels. Table 5 reports the alignment results for two representative models, the top-performing proprietary and open-source models on the GeoArena leaderboard, Gemini 2.5 Pro and Qwen2.5-VL-72B. The results show that Gemini 2.5 Pro achieves a substantially higher agreement rate (65.79%) with human evaluations compared to Qwen-VL-72B (46.67%). This suggests that Gemini 2.5 Pro exhibits stronger alignment with human judgment in assessing geolocalization task responses. In contrast, Qwen2.5-VL-72B demonstrates a lower consistency, indicating potential challenges in capturing the nuanced criteria (accuracy, evidence, and clarity) valued by human annotators. These findings highlight that while LLMs can approximate human preferences to a certain extent, significant gaps remain. This motivates future work on designing more faithful and robust LLM-based evaluators for geolocalization and other multimodal tasks.

4.5 CASE STUDY

To illustrate our framework, we present a case study using an image of the Ngātoroirangi Māori Rock Carvings at Mine Bay on Lake Taupō, New Zealand. As shown in Figure 1, different models exhibit varying levels of reasoning depth and factual accuracy. Gemini 2.5 Pro produces a comprehensive analysis, identifying salient visual features such as the Māori face carving, surrounding cliffs, and water-based accessibility, while also providing historical and cultural context (e.g., the carving’s creation in 1980 by Matahi Whakataka-Brightwell). In contrast, GPT-4o mini generates only a brief description, lacking explicit reasoning and omitting cultural details. This comparison underscores the importance of reasoning quality and contextual grounding in geolocalization tasks, showing that structured analyses align more closely with human preferences and task requirements. We also give hard cases analysis and more case studies in Appendix A.3 and Appendix A.4.

5 CONCLUSION

In this work, we present GeoArena, a live and human-centered benchmarking platform for evaluating large vision-language models on image worldwide geolocalization tasks. By collecting in-the-wild user-submitted images and integrating pairwise human preference evaluations, GeoArena overcomes the limitations of existing static benchmarks that often suffer from data leakage, insufficient reasoning assessment, and privacy issues. We implement a stable Bradley-Terry model, enabling reliable and interpretable ranking of models under diverse real-world conditions.

REFERENCES

Josh Achiam, Steven Adler, Sandhini Agarwal, Lama Ahmad, Ilge Akkaya, Florencia Leoni Aleman, Diogo Almeida, Janko Altenschmidt, Sam Altman, Shyamal Anadkat, et al. Gpt-4 technical report. *arXiv preprint arXiv:2303.08774*, 2023.

Guillaume Astruc, Nicolas Dufour, Ioannis Siglidis, Constantin Aronssohn, Nacim Bouia, Stephanie Fu, Romain Loiseau, Van Nguyen Nguyen, Charles Raude, Elliot Vincent, et al. Openstreetview-5m: The many roads to global visual geolocation. In *Proceedings of the IEEE/CVF Conference on Computer Vision and Pattern Recognition*, pp. 21967–21977, 2024.

Shuai Bai, Keqin Chen, Xuejing Liu, Jialin Wang, Wenbin Ge, Sibo Song, Kai Dang, Peng Wang, Shijie Wang, Jun Tang, et al. Qwen2. 5-vl technical report. *arXiv preprint arXiv:2502.13923*, 2025.

Rohan Bavishi, Erich Elsen, Curtis Hawthorne, Maxwell Nye, Augustus Odena, Arushi Somani, and Sağnak Taşırlar. Introducing our multimodal models, 2023. URL <https://www.adept.ai/blog/fuyu-8b>.

Ralph Allan Bradley and Milton E Terry. Rank analysis of incomplete block designs: I. the method of paired comparisons. *Biometrika*, 39(3/4):324–345, 1952.

Wei-Lin Chiang, Lianmin Zheng, Ying Sheng, Anastasios Nikolas Angelopoulos, Tianle Li, Dacheng Li, Banghua Zhu, Hao Zhang, Michael Jordan, Joseph E Gonzalez, et al. Chatbot arena: An open platform for evaluating llms by human preference. In *Forty-first International Conference on Machine Learning*, 2024.

Xiaoyi Dong, Pan Zhang, Yuhang Zang, Yuhang Cao, Bin Wang, Linke Ouyang, Xilin Wei, Songyang Zhang, Haodong Duan, Maosong Cao, et al. Internlm-xcomposer2: Mastering free-form text-image composition and comprehension in vision-language large model. *arXiv preprint arXiv:2401.16420*, 2024.

Yann Dubois, Balázs Galambosi, Percy Liang, and Tatsunori B Hashimoto. Length-controlled alpacaeval: A simple way to debias automatic evaluators. *arXiv preprint arXiv:2404.04475*, 2024.

Lukas Haas, Michal Skreta, Silas Alberti, and Chelsea Finn. Pigeon: Predicting image geolocations. In *Proceedings of the IEEE/CVF Conference on Computer Vision and Pattern Recognition*, pp. 12893–12902, 2024.

James Hays and Alexei A Efros. Im2gps: estimating geographic information from a single image. In *2008 ieee conference on computer vision and pattern recognition*, pp. 1–8. IEEE, 2008.

Kaiming He, Xiangyu Zhang, Shaoqing Ren, and Jian Sun. Deep residual learning for image recognition. In *Proceedings of the IEEE conference on computer vision and pattern recognition*, pp. 770–778, 2016.

Jingyuan Huang, Jen-tse Huang, Ziyi Liu, Xiaoyuan Liu, Wenxuan Wang, and Jieyu Zhao. Vlms as geoguessr masters: Exceptional performance, hidden biases, and privacy risks. *arXiv preprint arXiv:2502.11163*, 2025.

Neel Jay, Hieu Minh Nguyen, Trung Dung Hoang, and Jacob Haimes. Evaluating precise geolocation inference capabilities of vision language models. *arXiv preprint arXiv:2502.14412*, 2025.

Pengyue Jia, Yiding Liu, Xiaopeng Li, Xiangyu Zhao, Yuhao Wang, Yantong Du, Xiao Han, Xuetao Wei, Shuaiqiang Wang, and Dawei Yin. G3: an effective and adaptive framework for worldwide geolocalization using large multi-modality models. *Advances in Neural Information Processing Systems*, 37:53198–53221, 2024.

Junnan Li, Dongxu Li, Silvio Savarese, and Steven Hoi. Blip-2: Bootstrapping language-image pre-training with frozen image encoders and large language models. In *International conference on machine learning*, pp. 19730–19742. PMLR, 2023.

Ling Li, Yu Ye, Bingchuan Jiang, and Wei Zeng. Georeasoner: Geo-localization with reasoning in street views using a large vision-language model. In *Forty-first International Conference on Machine Learning*, 2024.

Lingyao Li, Runlong Yu, Qikai Hu, Bowei Li, Min Deng, Yang Zhou, and Xiaowei Jia. From pixels to places: A systematic benchmark for evaluating image geolocalization ability in large language models. *arXiv preprint arXiv:2508.01608*, 2025.

Haotian Liu, Chunyuan Li, Qingyang Wu, and Yong Jae Lee. Visual instruction tuning. *Advances in neural information processing systems*, 36:34892–34916, 2023.

Yi Liu, Junchen Ding, Gelei Deng, Yuekang Li, Tianwei Zhang, Weisong Sun, Yaowen Zheng, Jingquan Ge, and Yang Liu. Image-based geolocation using large vision-language models. *arXiv preprint arXiv:2408.09474*, 2024.

Gengchen Mai, Krzysztof Janowicz, Yingjie Hu, Song Gao, Bo Yan, Rui Zhu, Ling Cai, and Ni Lao. A review of location encoding for geoloc: methods and applications. *International Journal of Geographical Information Science*, 36(4):639–673, 2022.

Mark Steyvers, Heliodoro Tejeda, Aakriti Kumar, Catarina Belem, Sheer Karny, Xinyue Hu, Lukas Mayer, and Padhraic Smyth. The calibration gap between model and human confidence in large language models. *arXiv preprint arXiv:2401.13835*, 2024.

Richard Szeliski. *Computer vision: algorithms and applications*. Springer Nature, 2022.

Gemini Team, Rohan Anil, Sebastian Borgeaud, Jean-Baptiste Alayrac, Jiahui Yu, Radu Soricut, Johan Schalkwyk, Andrew M Dai, Anja Hauth, Katie Millican, et al. Gemini: a family of highly capable multimodal models. *arXiv preprint arXiv:2312.11805*, 2023.

Gemma Team, Aishwarya Kamath, Johan Ferret, Shreya Pathak, Nino Vieillard, Ramona Merhej, Sarah Perrin, Tatiana Matejovicova, Alexandre Ramé, Morgane Rivière, et al. Gemma 3 technical report. *arXiv preprint arXiv:2503.19786*, 2025.

Bart Thomee, David A Shamma, Gerald Friedland, Benjamin Elizalde, Karl Ni, Douglas Poland, Damian Borth, and Li-Jia Li. Yfcc100m: The new data in multimedia research. *Communications of the ACM*, 59(2):64–73, 2016.

Wei-Lin Chiang Tianle Li, Anastasios Angelopoulos. Does style matter? disentangling style and substance in chatbot arena, August 2024. URL <https://blog.lmarena.ai/blog/2024/style-control/>.

Hugo Touvron, Thibaut Lavril, Gautier Izacard, Xavier Martinet, Marie-Anne Lachaux, Timothée Lacroix, Baptiste Rozière, Naman Goyal, Eric Hambro, Faisal Azhar, et al. Llama: Open and efficient foundation language models. *arXiv preprint arXiv:2302.13971*, 2023.

Vicente Vivanco Cepeda, Gaurav Kumar Nayak, and Mubarak Shah. Geoclip: Clip-inspired alignment between locations and images for effective worldwide geo-localization. *Advances in Neural Information Processing Systems*, 36:8690–8701, 2023.

Senzhang Wang, Jiannong Cao, and S Yu Philip. Deep learning for spatio-temporal data mining: A survey. *IEEE transactions on knowledge and data engineering*, 34(8):3681–3700, 2020.

Xiao Wang, Guangyao Chen, Guangwu Qian, Pengcheng Gao, Xiao-Yong Wei, Yaowei Wang, Yonghong Tian, and Wen Gao. Large-scale multi-modal pre-trained models: A comprehensive survey. *Machine Intelligence Research*, 20(4):447–482, 2023.

Zhiqiang Wang, Dejia Xu, Rana Muhammad Shahroz Khan, Yanbin Lin, Zhiwen Fan, and Xingquan Zhu. Llmgeo: Benchmarking large language models on image geolocation in-the-wild. *arXiv preprint arXiv:2405.20363*, 2024.

Jason Wei, Xuezhi Wang, Dale Schuurmans, Maarten Bosma, Fei Xia, Ed Chi, Quoc V Le, Denny Zhou, et al. Chain-of-thought prompting elicits reasoning in large language models. *Advances in neural information processing systems*, 35:24824–24837, 2022.

Wayne Xin Zhao, Kun Zhou, Junyi Li, Tianyi Tang, Xiaolei Wang, Yupeng Hou, Yingqian Min, Beichen Zhang, Junjie Zhang, Zican Dong, et al. A survey of large language models. *arXiv preprint arXiv:2303.18223*, 1(2), 2023.

Zhongliang Zhou, Jielu Zhang, Zihan Guan, Mengxuan Hu, Ni Lao, Lan Mu, Sheng Li, and Gengchen Mai. Img2loc: Revisiting image geolocalization using multi-modality foundation models and image-based retrieval-augmented generation. In *Proceedings of the 47th international acm sigir conference on research and development in information retrieval*, pp. 2749–2754, 2024.

A APPENDIX

A.1 DATASET CHARACTERISTICS AND COMPOSITION

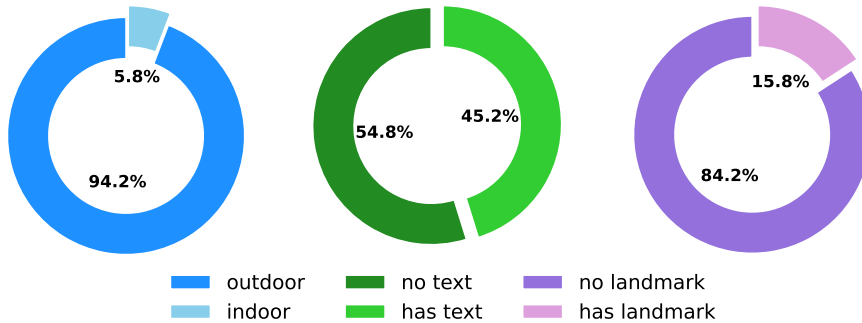


Figure 5: Composition of Image Features in GeoArena-1K Dataset

To further explore the characteristics of the GeoArena-1K dataset, we employ GPT-4o to annotate the collected images, focusing on three key aspects:

1. whether the image depicts an indoor or outdoor setting.
2. whether the image contains prominent, recognizable text.
3. whether the image features a landmark, such as a historical site or natural icon.

The corresponding results are presented in Figure 5. The figure comprises three doughnut charts, each illustrating the distribution of one of the annotated attributes across the GeoArena-1K dataset: Indoor/Outdoor Distribution:

1. The first doughnut chart indicates that 94.2% of images are classified as outdoor scenes, with only 5.8% representing indoor environments. This pronounced skew toward outdoor imagery aligns with the global scope of GeoArena, where user-submitted images are likely dominated by exterior scenes captured in diverse geographic contexts.
2. Text Presence: The second doughnut chart reveals a more balanced distribution, with 54.8% of images lacking recognizable text ("no text") and 45.2% containing text ("has text"). This near-equitable split underscores the dataset's richness, incorporating both text-free natural scenes and images with textual elements such as signs or labels. This variability is particularly valuable for assessing LVLM capabilities in multi-modal reasoning, where text recognition can enhance location prediction accuracy.
3. Landmark Presence: The third doughnut chart shows that 84.2% of images do not contain landmarks ("no landmark"), while 15.8% do ("has landmark"). The low prevalence of landmarks reflects the dataset's emphasis on general geographic scenes rather than iconic or tourist-heavy locations, offering a broad representation of natural and urban environments worldwide. This distribution highlights GeoArena-1K's potential to test LVLM generalization across less distinctive locales, a challenging yet realistic scenario for global geolocalization. Overall, these distributions reveal the GeoArena-1K dataset's heterogeneity, making it a robust resource for benchmarking LVLM performance under real-world conditions.

A.2 LVLM ALIGNMENT EVALUATION PROMPT

The prompt template used for LVLM alignment evaluation is as follows:



Figure 6: Case Study: Images Where Strong Models Excel but Weaker Models Fail

You are an expert evaluator in image geolocation tasks. I will give you two model responses to the same geolocation prompt.

Here is the prompt:

- Prompt: {sample['prompt']}
- Image: {sample['image']}

Response A: {sample['response A']}

Response B: {sample['response B']}

Your task is to decide which response is better based on:

1. Accuracy of the predicted location
2. Strength of reasoning and evidence
3. Clarity and specificity

Output only one word:

- “win” if Response A is better
- “loss” if Response B is better
- “tie” if both are equally good

We first prompt the LVLM to act as an expert evaluator for the geolocalization task. For each sample, the model is provided with the prompt and the associated images, along with the responses from two candidate models. It is then asked to determine which response is better, considering three dimensions: accuracy, reasoning, and clarity and specificity.

A.3 HARD CASES ANALYSIS

To better understand the distinction between top-tier and lower-tier models, we examined a set of representative cases where strong models predicted correctly but weaker models failed, as illustrated in the Figure 6. Specifically, we selected the top-5 models on the leaderboard—Gemini-2.5-Pro, Gemini-2.5-Flash, Qwen2.5-VL-72B-Instruct, Gemma-3-12B-it, and Gemma-3-27B-it—as well as the bottom-5 models—GPT-4o, LLaMA-4-Scout, Qwen2.5-VL-7B-Instruct, GPT-4.1-Nano, and GPT-4o-Mini. We then extracted examples where the top-5 models outperformed the bottom-5 models. These images generally do not contain prominent or unique landmarks that can be easily recognized. Instead, they often depict environments that require reasoning over subtle contextual cues—such as vegetation types, architectural style, road structures, or geographic textures—to infer the location. This suggests that strong models may better leverage fine-grained reasoning and background knowledge beyond surface-level features. The presence of such challenging samples highlights a promising direction for future model development: expanding training and evaluation on these harder

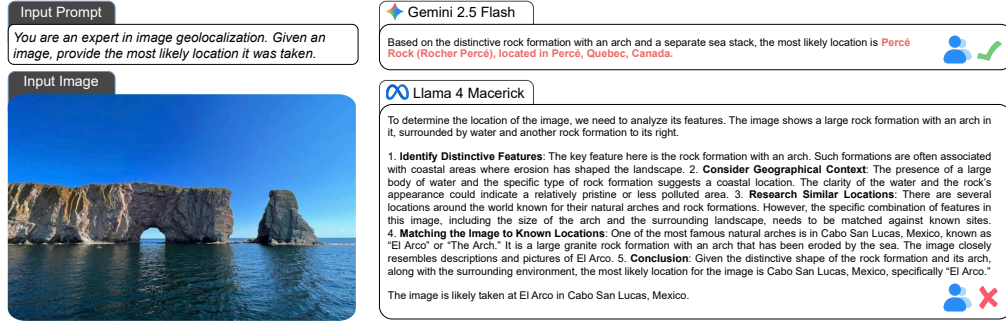


Figure 7: Additional Case Study: Identifying the Percé Rock.



Figure 8: Additional Case Study: Identifying the Olympic Park, Beijing.

cases. By doing so, upcoming systems may gain robustness and achieve more consistent performance across diverse scenarios, particularly where visual clues are subtle and non-obvious.

A.4 ADDITIONAL CASES FROM GEOARENA

In this section, we present additional case studies from GeoArena to illustrate the diversity and complexity of the geolocalization tasks it encompasses. Figure 7 showcases an image of the iconic Percé Rock in Quebec, Canada, highlighting the model's ability to recognize unique geological formations. Figure 8 features the Olympic Park in Beijing, China, demonstrating the model's proficiency in identifying modern architectural landmarks. Lastly, Figure 9 depicts a golf course in Fiji, emphasizing the model's capability to infer locations based on environmental and recreational context. These examples underscore GeoArena's effectiveness in challenging models to perform accurate geolocalization across a wide range of scenarios.

Input Prompt

You are an expert in image geolocalization. Given an image, provide the most likely location it was taken.

Input Image



Llama 4 Macerick

Based on the image provided, the landscape depicted appears to be a tropical or subtropical region, characterized by a golf course, dense vegetation, and a coastline with clear turquoise water.

1. **Climate and Vegetation:** The presence of dense lush greenery and palm trees indicates a tropical or subtropical climate. Regions known for such landscapes include parts of the Caribbean, Southeast Asia, and the Pacific Islands. 2. **Golf Course and Infrastructure:** The well-maintained golf course and surrounding infrastructure (e.g., buildings along the coast) suggest a popular tourist destination. Many tropical and subtropical regions have developed golf courses and resorts to attract tourism. 3. **Coastline and Water Characteristics:** The clear turquoise water and the coral reef visible in the shallow waters are characteristic of tropical marine environments. This feature is common in areas like the Caribbean and the Pacific Islands. 4. **Specific Location Clues:** Without specific landmarks or text, we rely on the overall aesthetic and features. However, the layout of the golf course, the vegetation, and the clarity of the water can sometimes give clues. For instance, the presence of a fringing reef is typical of many Pacific Island locations.

Given these observations, a plausible location for this image could be in the Pacific Islands or the Caribbean. However, without more specific details or recognizable landmarks, pinpointing the exact location is challenging. That said, one of the locations that closely match the description and the visual characteristics is **Fiji**. Fiji is known for its clear waters, coral reefs, lush vegetation, and numerous golf courses and resorts, making it a popular destination for both golfing and beach tourism.

In conclusion, while the exact location cannot be determined with absolute certainty without additional information, **Fiji is a strong candidate based on the visual cues provided in the image.**



Gemma 3 12b

Okay, let's analyze this image and pinpoint its likely location. Here's my assessment based on visual cues and my expertise in image geolocalization:

Most Likely Location: **Kempinski Grand Bale, Mauritius**

Reasoning: 1. **Vegetation and Landscape:** The lush, tropical vegetation (palm trees, dense foliage) immediately points to a tropical location. 2. **Golf Course:** The presence of a well-manicured golf course is a significant clue. This is not just anywhere; it's a high-end resort area. 3. **Turquoise Water and Barrier Reef:** The incredibly clear, turquoise water and the visible barrier reef are crucial. The color and clarity of the water suggest a specific type of coral reef environment. 4. **Coastal Architecture:** The buildings along the coast feature a distinctive architectural style often seen in luxury resorts. 5. **Match with known Images of the Kempinski Grand Bale:** The layout of the golf course and coastline, revegetation, and building styles strongly match aerial views and images of the Kempinski Grand Bale resort in Mauritius. The resort has a unique course with distinctive features.

Further refinements: Based on the elevation and angle of the photograph, the photo was likely taken from a drone.

Confidence Level: 95%

Disclaimer: While I am highly confident, certain features can change slightly over time, and other locations could theoretically exhibit similar characteristics. However, the combination of factors makes Kempinski Grand Bale the most probable location.

If you have other images you'd like me to analyze, please send them over!



Figure 9: Additional Case Study: Identifying the Golf Course in Fiji.